

## On the Interface Between LENS® Deposited Stainless Steel 304L Repair Geometry and Cast or Machined Components

D. D. Gill, J. E. Smugeresky, M. F. Harris, C. V. Robino, M. L. Griffith  
Sandia National Laboratories\*  
Albuquerque, NM 87185

### Abstract

Laser Engineered Net Shaping™ (LENS®) is being evaluated for use as a metal component repair/modification process. A component of the evaluation is to better understand the characteristics of the interface between LENS deposited material and the substrate on which it is deposited. A processing and metallurgical evaluation was made on LENS processed material fabricated for component qualification tests. A process parameter evaluation was used to determine optimum build parameters and these parameters were used in the fabrication of tensile test specimens to study the characteristics of the interface between LENS deposited material and several types of substrates. Analyses of the interface included mechanical properties, microstructure, and metallurgical integrity. Test samples were determined for a variety of geometric configurations associated with interfaces between LENS deposited material and both wrought base material or previously deposited LENS material. Thirteen different interface configurations were fabricated for evaluation representing a spectrum of deposition conditions from complete part build, to hybrid substrate-LENS builds, to repair builds for damaged or re-designed housings. Good mechanical properties and full density were observed for all configurations. When tested to failure, fracture occurred by ductile microvoid coalescence. The repair and hybrid interfaces showed the same metallurgical integrity as, and had properties similar to, monolithic LENS deposits.

### Introduction

Laser Engineered Net Shaping™ (LENS®) is a laser metal deposition process developed at Sandia National Laboratories. The process is capable of depositing many types of metal onto substrates using a laser. With the proper process parameters, LENS depositions can be composed of fully dense material with properties similar or superior to that of wrought materials. The ability of LENS to deposit freeform structures on metal substrates makes this process an ideal candidate for the repair of castings and machined structures. This study focuses on the initial requirement for a precision repair system; the understanding of the interface between the deposited material and the substrate whether that substrate is cast, wrought, or previously deposited LENS material. For this investigation 304L stainless steel was chosen. Studies performed for the research included a process parameter study to determine the optimum processing window for the material, the creation of a set of representative geometry samples deposited on different substrates, the machining of these samples into tensile test specimen, and tensile testing of the samples followed by metallographic analyses.

\* Sandia is a multiprogram laboratory operated by Sandia Corporation, a Lockheed Martin Company, for the United States Department of Energy's National Nuclear Security Administration under Contract DE-AC04-94AL85000.

## Process Parameter Testing

LENS has the ability to not only create geometry, but also, to a certain extent, control the material properties by varying the process parameters associated with the deposition of powdered metal onto substrates. Different process parameters affect the deposition characteristics and material microstructure, therefore varying the material properties. Because of this ability, it is important to test process parameters carefully for each material. The LENS process creates a pool of molten metal where the laser is focused onto a metal substrate. Powdered metal is then blown into the weld pool to create a small deposit. The substrate is moved in a plane perpendicular to the laser axis creating a line of deposited metal. Many lines near each other create a layer, and as the process is repeated with the laser focal point at increasing heights off the substrate, a part is built line by line, and layer by layer. The commonly adjusted LENS process parameters, as shown in Figure 1, are laser power, feedrate of the axes which move the substrate, hatch width, layer thickness, and metal powder mass flow rate. The process variable “hatch width” refers to the distance between parallel passes of the laser as it rasters back and forth to fill in the interior of a geometry. The layer thickness is the amount that the height of the laser focal point is raised from one layer to the next.

A sample coupon size that has been found to work well for process parameter testing is  $\frac{1}{2} \times \frac{1}{2} \times \frac{1}{2}$  inch cubes. These cubes are large enough to exhibit the characteristics of larger block-like solid features, but small enough to be built relatively quickly. For this test, 42 blocks were built with different parameter combinations and the blocks were measured for height and appearance, and then some were sectioned and polished to determine the porosity and microhardness of the block's interior. A test matrix of 9 cubes deposited on a  $\frac{1}{4}$ " thick substrate is shown in Figure 2 with 3 of the cubes having been sectioned, potted, and polished.

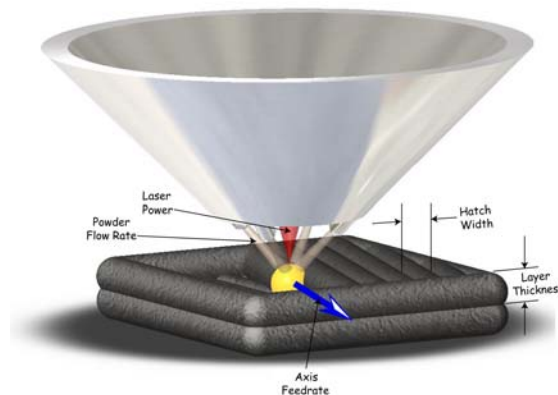


**Figure 1.** A Model of the LENS Metal Deposition Process Showing Process Parameters That Are Utilized to Select Build Characteristics.

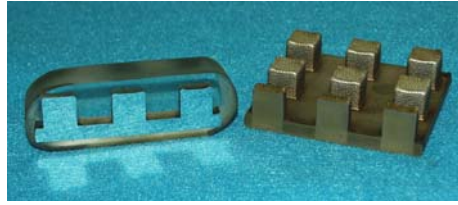


**Figure 2.** Test Matrix of 9 LENS Deposited Cubes Showing 3 Cubes that Have Been Sectioned, Potted, and Polished for Additional Analysis.

The process parameters that were varied for these tests were the hatch width (distance between successive line deposits), layer thickness, powder mass flow rate, and axis feedrate. The values used for each of these parameters are shown in Table 1.

**Table 1.** Process Parameters and Parameter Values Used in Testing.

Parameter	Values Used in Parameter Test
Hatch Width (inches)	0.020", 0.024", 0.030"
Layer Thickness (inches)	0.025", 0.030"
Powder Mass Flow Rate (grams per min.)	21.8-57.7gpm
Axis Feed Rate (inches per min.)	20ipm, 25ipm, 30ipm

Other machine parameters were held constant for all of the testing. These parameters include layer thickness and the parameters in the system that controls the weld pool area. All cubes were deposited evenly spaced on SS304L substrates 1/4" thick and approximately 3x3" square.

### Analysis and Results

After all of the cubes had been deposited using different combinations of process parameters, the analysis of each cube included build height and appearance. Though a subjective measurement, the cube appearance has been found to be a good first pass indication of the quality of the build. Good process parameter sets produce cubes with sharp corners, flat tops, and finely visible hatch lines across the top and sides. A second measure is the ability of the parameter set to produce a cube that builds to the design height or above. Because LENS is a near net-shape process and stock will have to be machined away in future processing steps, it is desirable that the outside dimensions of the deposited feature be equal to or greater than the design dimensions leaving machining stock. The cubes that built to or above design height were cut in half vertically using a wire EDM. These cubes were then potted, polished, and examined to determine the porosity of each cube.

The effects of different factors were compared by measuring the part porosity, microhardness, and build height. Due to constraints on resources, only 17 of the 42 cubes were sectioned and examined for porosity. Five of the sectioned cubes were tested for microhardness. Four cubes that were as high or higher than the design height and had good appearance were chosen to be sectioned and hardness tested. As is seen in Figure 2, it is as easy to section and polish an entire row of 3 cubes as it is to use a single cube. This accounts for the difference between the number of cubes that were sectioned and the number that were tested for microhardness.

The porosity was measured by manually counting the number of pores visible in an optical microscope at 50x magnification which gives a visible area of 500µm x 500µm. The pores were

divided into two groups, those with diameters of 1-5 $\mu\text{m}$ , and those with diameters of 6-15 $\mu\text{m}$ . For the samples with the highest porosity, the number of pores was counted for a smaller area and then extrapolated as an estimate of the number of pores in the entire area. The porosity was then compared with the process variables hatch width, axis feedrate, and powder mass flow rate individually. None of these comparisons showed a statistically significant correlation with the porosity. However, it was determined that the number of pores appears to depend on a richness factor. The richness factor is defined as the ratio of the powder feedrate to the product of the hatch width, axis feedrate, and layer thickness. The units of the richness factor are  $\text{g/in}^3$  which represents the richness, or the mass of powder per unit volume to be filled by that powder. As the richness factor increases there is more powder supplied to fill a certain volume of build space. As is shown in Figure 3a, when the richness factor is higher, the number of large pores decreases, but the number of small pores increases.

The proposed explanation is that at high powder flow rates, the weld pool is overwhelmed with powder and is not able to fully melt all of the incoming powder that leaves small voids in the material. When the richness factor is low, there is a shortage of powder and the weld pool is somewhat starved for powder. In previous work, it has been noted that the melted powder attempts to draw into a ball due to the surface tension of the material. It appears that the powder starvation in the weld pool allows the material to pull apart leaving the larger 6-15 $\mu\text{m}$  voids. It is important to note that even in the sample with the greatest number of large pores, there were still only 5 large pores in the 500 $\mu\text{m}$  x 500 $\mu\text{m}$  area. The majority of the area vacated due to porosity is due to the small pores. The small pores occupy between 0.07% and 10% of the total area in the samples as is shown in Figure 3b. Comparing the blue diamonds in graphs 3a and 3b, it is evident that the majority of the area vacated due to porosity is due to the smaller pores.

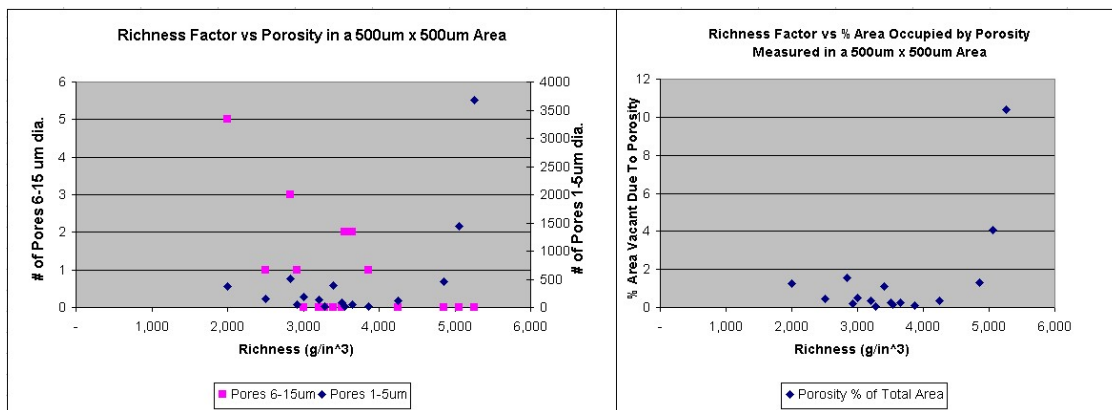


**Figure 3.** Richness Factor Compared with Porosity by Pore Size(a) and by Percent of Total Area Consumed By Pores(b).

The microhardness measured in the 4 samples was found to be fairly consistent between the samples with no assignable variation due to the deposition factors. The micro hardness was measured in 5 locations on each of the 4 samples. The average hardness of the cubes ranged between 176 and 195 Vickers hardness, but the one standard deviation error bars showed that the mean values of microhardness for each cube are not significantly different than the other cubes.



deposited material and a wrought material substrate (parts D, E, F, G, H, M). The third group has an interface between two sets of LENS material deposited in different orientations (parts J, K, L, N). To make the samples more realistically representative of 3 dimensional LENS repair and modification, the angle of the interface was tested at both 90° (parts D, E, F, L, M, N) and at 45° (parts G, H, J, K.) A 90° interface causes the newly built layers to be parallel to the interface which is a good means of testing inter-layer adhesion. The 45° interface causes each LENS deposited layer to be slightly longer than the previous layer. Thus, each layer's interaction with the interface contains an "end" where the weld pool is stopped and started again as the machine axes change the feed direction. The ends of layers might be suspected as being the most susceptible region for porosity and bond weakness. An additional test is shown in part M in which the substrate is integral to, and becomes part of, the final component. This sample has two interfaces created at different times.

For the Block Tower or thick features, sample sets B and C represent monolithic vertical and horizontal LENS™ builds respectively. Sample sets D and G represent interfaces of a LENS™ deposit onto a bulk wrought substrate, the former oriented 90° and the latter 45° to the build direction. Sample set M represents interfaces of a LENS™ deposit onto opposite sides of a bulk wrought substrate at 90°. Sample sets L and J represent interfaces of a LENS™ deposit onto a previously fabricated LENS™ deposited substrate, the former with an interface oriented 90° and the latter with an interface oriented 45° to the build direction.

For the Thin Wall Builds, sample set A represents monolithic deposits. Sample sets E, and H represent LENS™ deposits on thin walled wrought substrates with 90° and 45° interfaces respectively, and set F represents a thin wall into a more massive substrate. Sets K and L represent LENS™ walls deposited onto previously deposited thin LENS™ walls at 45° and 90° interfaces respectively.

The coupons built as tension test sample were deposited using the parameters determined in the process parameter test. These parameters were 0.020" hatch width, 0.020" layer thickness, 20ipm feedrate, 23g/min powder flow rate, and a laser power controlled by the automated weld pool area control between 400-700 Watts for the block/tower geometry. The thin walls structures were built with the same process parameters except that the powder flow rate was 20.3g/min and the laser power modulated between 26-31Amps. The hatch travel direction for each successive layer was rotated 105 degrees. On the thin wall samples, the fewest number of line scans per layer is 5 (3 hatch + 2 border) and the maximum number of scans is 49 (47 hatch + 2 border), depending on deposition direction. For the chosen test types, either 2 or 3 tensile specimen were created. The LENS deposited samples are shown in Figure 6.

As can be seen in Figure 5, not all of the coupons were deposited perfectly, especially with respect to alignment. Most of the misalignments were due to difficulties fixturing a previously deposited LENS sample for subsequent processing. However, the misalignment of the deposited sections was seen as acceptable due to the machining of each sample into a tension test specimen. For the tension test, the parts were machined significantly, especially in the area of the interface. At these areas, the parts were machined to have significantly reduced cross section to focus the stress around the interface. This reduction in cross section effectively machined away any misalignment. Careful notes were taken during the LENS building process especially

to record any processing anomalies that might have an effect on the strength of the parts and interfaces between sections. The samples were made from gas atomized 304L stainless steel powders.

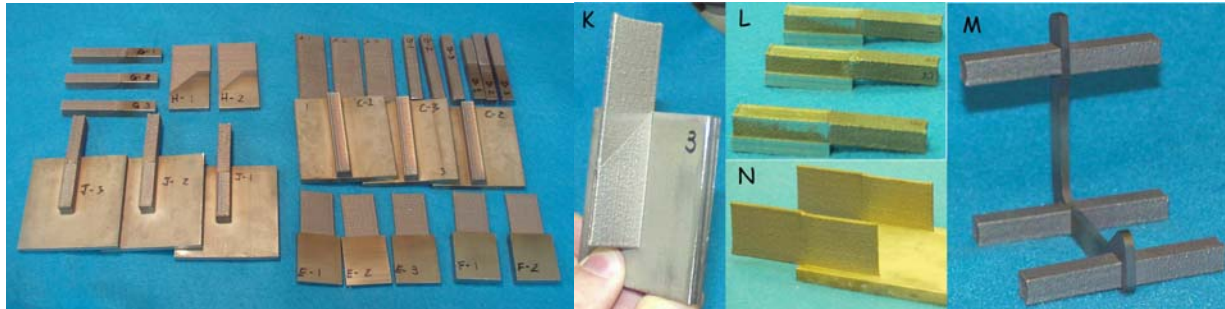


**Figure 5.** LENS Deposited Sample Types A-N for Machining Into Tensile Specimens.

### **Tension Test Experimental Procedures**

The deposited LENS samples were sectioned by EDM for metallographic mounting and/or for further machining into tensile bars for mechanical testing. The metallographic samples were taken from the top of each LENS deposited region with the cut oriented perpendicular to the final layer deposition direction. This cut provides a view that allows an assessment of the melt pool size, relative amounts of overlap of successive deposit traces into the plane of the sample, and amount of re-melt of each successive layer. Round tensile bars with a 0.125 inch diameter and 0.5 in gage length were used for the tower/bulk deposited material and flat tensile samples 0.020 inches thick by 0.063 inch wide with a 0.5 inch gage length were used for the thin wall configuration. A knife-edge extensometer was used on the round samples, and a laser extensometer was used on the flat samples. The samples were strained using the standard 0.2 inches per minute cross head speed. The ultimate tensile strength, yield strength, elongation and reduction in area were determined. Both smooth and notched samples were evaluated. In order to assess interface characteristics, the notched samples were machined to bias the loading such that the fracture would initiate as close to the interface as possible. Strength values were determined by the usual analysis of the stress strain curves for both smooth and notched samples. However, values for notched samples are not representative of the actual strengths, and were only used for comparing relative strengths of the notched samples. Ductility as measured by reduction of area (RA) was expected to be similar for notched and un-notched samples. In turn, these represent a range of interfaces expected for building cantilevered or repair extensions on damaged parts.

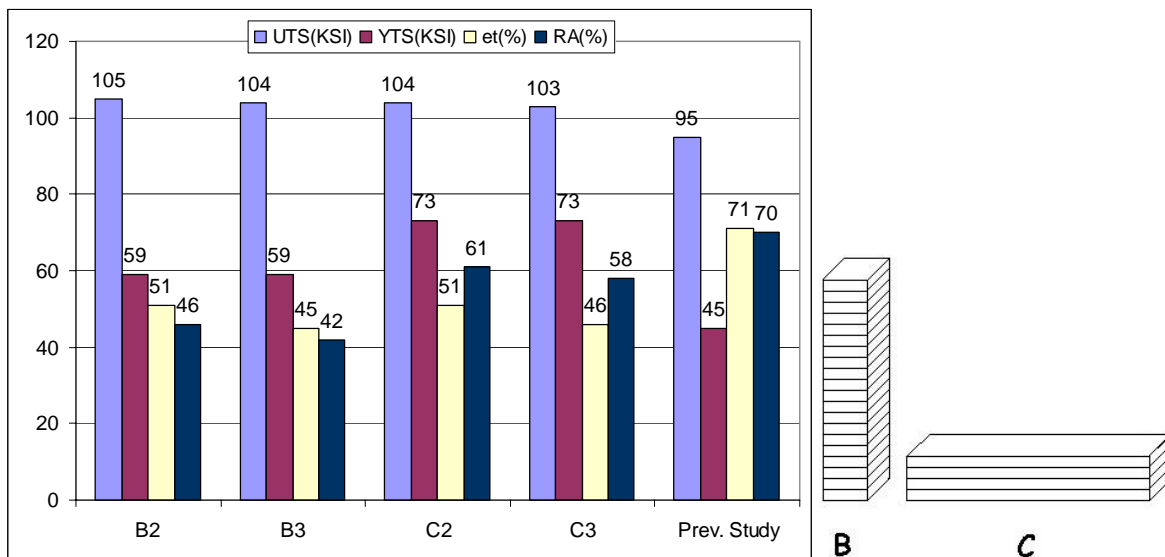
Metallographic samples were mounted in clear epoxy and prepared using standard metallographic grinding and polishing techniques. Etching was done using an electrolytic oxalic etch at 3 V for 15 seconds. Samples were examined optically for porosity to assess their metallurgical integrity, and the amounts of re-melt with each pass and/or layer. A qualitative assessment of the fracture behavior was done using SEM observations of one half of a subset of the fractured tensile samples.



## Results and Discussion

Observations are made for each of the basic types of deposition: 1) Complete or monolithic LENS part builds, 2) Hybrid LENS builds onto an integral wrought/cast substrate; and 3) Repair or re-construction LENS builds on damaged or salvaged housings. The tensile results for smooth bar samples are shown in Figures 7 and 8. The values listed in these figures are ultimate tensile strength (UTS), tensile yield strength (YTS), tensile elongation (et), and reduction in area (RA).

Figure 7 shows the Monolithic Block/Tower LENS build properties. The yield strengths for the vertical tower builds (type B) were 59 KSI, and ductility measured by elongation of 45% and 51%, while ductility measured by reduction in area were 42% and 46%. Yield strengths for the horizontal block builds (type C) were 73 KSI, and ductility measured by elongation were 46% and 51%, while ductility measured by reduction in area were 61% and 58%. The yield strengths for a previous in-house study of LENS deposited 304 stainless steel Tower Builds were only 45 KSI, but with a higher ductility of about 70%, for both elongation and reduction of area.



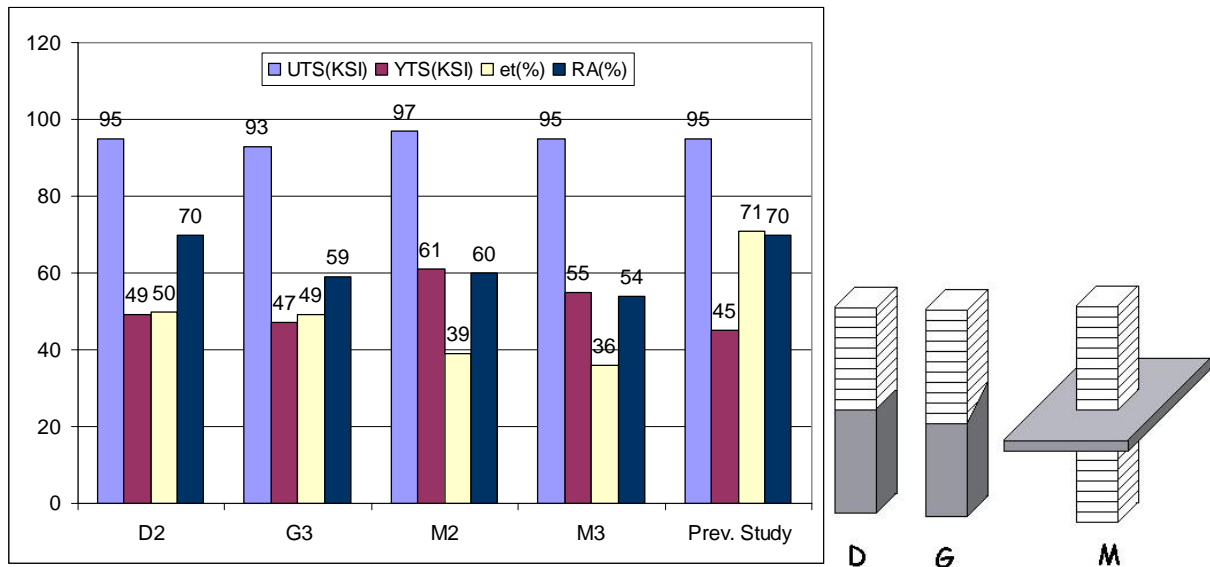
**Figure 7.** Mechanical Properties of Monolithic LENS Builds Comparing Block Tower Geometry (Types B and C) to a Previous Study for 304SS.

Figure 8 shows properties of the Hybrid Block/Tower LENS built geometry on wrought or cast substrates. The yield strengths for the hybrid LENS builds on wrought substrates ranged from 47 to 61 KSI, and ductility measured by elongation ranged from 36% to 50%, while ductility measured by reduction in area ranged from 54% to 70%. The yield strengths for the single interface samples, D and G, were lower than the yield strengths for the double interface set M. The single interface values are comparable to those of a previous in-house study of monolithic LENS™ deposited 304 stainless steel Tower Builds. However, the ductility as measured by elongation was lower. There is an indication that the orientation of the interface may affect the measured ductility, (higher for 90° than for 45°) but not the strength.

Figure 9 shows the properties of hybrid LENS Thin Wall builds on wrought or cast substrates for notched flat tensile specimens. For the flat specimens, much lower loads were needed to reach the yield and fracture strengths, and consequently this data had more uncertainty because it used



the lower end of the load cell range. Sample sets E and F represent differences in mass of the substrate on a thin wall to substrate interface, and therefore different cooling rates at the interface. The more massive substrate interface had a slightly higher yield strength, but the same ductility as measured by elongation. Sample set H had both a 90° and a 45° interface, with the 90° interface having a lower yield strength and the 45° interface having about the same strength as the E and F sets. For reference, the notched samples are compared to the LENS-on-LENS thin wall set N for which both notched and smooth samples were tested. The smooth samples from set N have total elongations greater than 20%, compared to the notched sample with 10%. Again, the values for yield strength and total elongation of the notched samples are not valid values but give relative indications of differences between samples. We see here that the strengths of interfaces between hybrid LENS on wrought substrates is lower than the strengths of interfaces between LENS on LENS substrates. The differences in ductility between the two types of build may be due to the specimen geometry, but determination was outside the scope of this study.



**Figure 8.** Mechanical Properties of Hybrid LENS Block Tower Builds on Wrought Substrates Comparing Sample Types D, G, and M to a Previous Study for 304SS.

Figure 10 shows the properties of LENS builds on previously built LENS substrates, comparing Block Tower types (samples L and J) to Thin Wall types (samples N and K). Round tensile bars were used for the Block Tower builds and thin flat tensile bars for the Thin Wall builds. Yield strengths ranged from 64 to 71 KSI for the Block tower builds and from 52 to 70 KSI for the Thin Wall builds. As was the case for monolithic LENS samples, the strengths of the two different types of build as measured on two different sample geometries were similar, but the total elongations were lower for the flat specimens. The values compare favorably with monolithic LENS deposited material.

In general, the strengths of the smooth round tensile bars are about twice that of annealed material, but without any significant difference in ductility. These values represent enhancements to annealed 304L stainless steel and give designers a higher strength material, without needing to work it or having to switch to age-hardenable compositions that would

require post shaping heat treatments. While not the same range of strengths as alloys like PH13-8 Mo, the LENS processed material offers a lower cost alternative which would also eliminate the need for heat treatment.

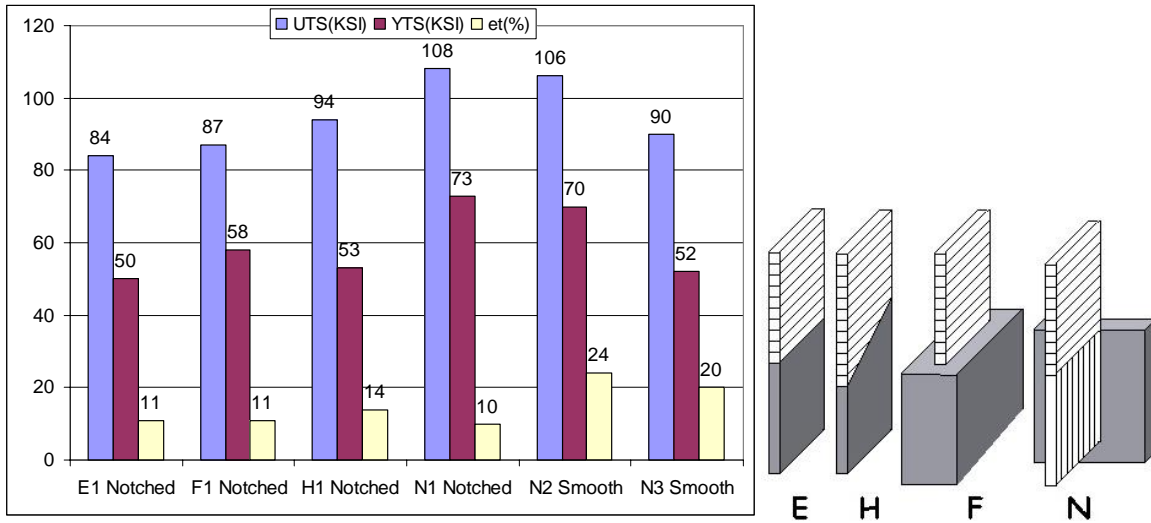


**Figure 9.** Mechanical Properties of Hybrid LENS Thin Wall Builds on Wrought Substrates Comparing Sample Types E, H, and F to Sample Types N Deposited on LENS Substrates.

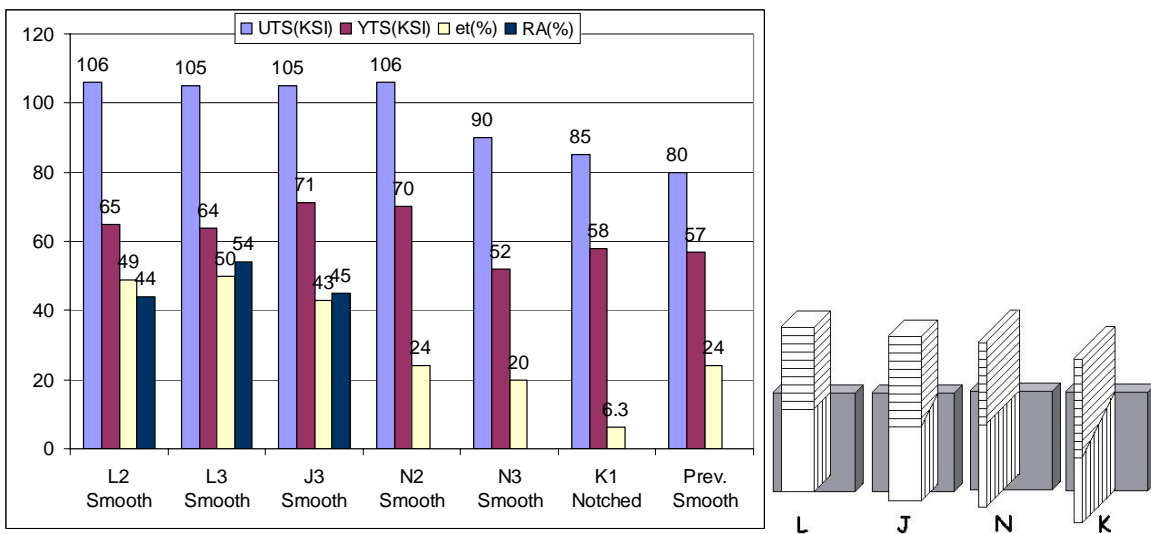


**Figure 10.** Mechanical Properties of LENS Builds on Previously Deposited LENS Substrates of Types L and J (Block Tower) Compared to N and K (Thin Wall) and a 316 SS Thin Wall From a Previous Study.

The microstructure of all samples contains features at two size scales. At the largest size scale are boundaries that result from overlapping passes in the same plane (inter-pass boundaries) as well as boundaries formed by successive layers (interlayer boundaries). These correspond to the molten metal pool size, which depends upon the deposition conditions. The microstructure shows some minor closed porosity. At higher magnifications, finer microstructural features which are likely  $\delta$ -ferrite are observed with multiple orientation variants at the interfaces between successive overlapping line passes and layers. The ferrite has a lath-like morphology that gives a needle-like appearance if viewed transversely. There is both an epitaxial

solidification component as well as the more orthogonal component of the interface microstructure, as shown in Figure 11. In general, there is complete filling of void space for all samples examined. The occasional closed pores do not appear to strongly impact the tensile strength or ductility, and it is believed that porosity levels can be reduced through further process optimization.

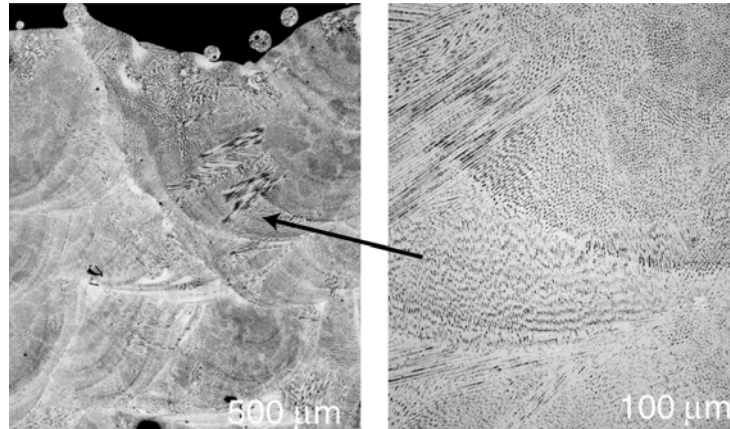


**Figure 11.** Details of Microstructure at the Top of a Type N Thin Wall Sample.

A fracture surfaces from sample M is shown in Figure 12 and is representative of fracture surfaces seen on most of the samples tested. However, the fracture surfaces of sample L showed some unusual features for several samples, apparently associated with inadequate lack of fusion across interfaces associated with the interrupted deposition of material required to examine repair scenarios and extended cantilever builds.

Fracture surfaces in general consist of macroscopic cup-cone fracture, and a microscopic ductile dimpled fracture mode. These features are similar to that observed in wrought material fracture, except that the LENS deposits also occasionally exhibited secondary features corresponding to irregularities in deposition layer spacing. Figure 12 shows the ductile fracture features for a type M LENS feature built on both sides of a wrought substrate. The figure shows the characteristic cup-cone features in the low magnification images and ductile dimpled features at higher magnification. The ductile dimple features are seen in a mixture of dimple sizes with some evidence of secondary cracking. The ductility of this sample was 36% total elongation. In a few cases, defects that are thought to be due to lack of fusion were observed. These were all identified as deposits that had experienced disruptions during the deposition process. The ductility of these samples was still of similar total elongation to the other samples, indicating that measured ductility does not significantly reflect changes in the nature of the fracture features.



**Figure 12.** Fracture Surface of a Type M LENS Build on Both Sides of a Wrought Substrate.

## **Summary and Conclusions**

The tensile data for smooth tensile bars indicates good metallurgical bonding between LENS® deposits and the substrates for the range of configurations studied. The yield strengths are substantially higher than a previous study of 304L stainless steel, and they are more like those reported for 316 stainless steel. This means that for both 316 and 304 stainless steels, it is possible to obtain LENS deposited material with about twice the strength as annealed wrought bar, but with no significant reduction in ductility, as is observed for the work hardened condition of wrought bar stock. Notched samples were also tested to force fracture at the interface between LENS deposit and substrate, and no differences in fracture mode from that of smooth tensile samples was observed. There were no significant differences in ductility from one sample to another or for duplicate samples, but there were some noticeable differences in fracture characteristics when examined in the SEM. Fracture, in all cases, is by ductile microvoid coalescence and based on matches of the periodicity of the fracture feature and the periodicity of the interlayer interfaces, the differences appear to coincide with evidence of premature separation at inter-layer boundaries. In turn, these differences corresponded to documented abnormalities in the baseline deposition parameters. Samples not experiencing abnormalities in processing conditions did not exhibit this particular feature. By insuring that closed loop feedback control of the melt pool during deposition is engaged, the above mentioned types of abnormality are not expected to occur.

The microstructure was typical of previously characterized fully dense LENS deposits. The cross sections perpendicular to the deposition direction allow metallographic analysis of melt pool size and both interlayer and inter-pass overlaps. All samples exhibited adequate overlap to insure complete filling of void space, and complete melting and re-solidification of the feedstock. However, there were two irregularities: 1) The overlaps, although adequate, were not as uniform as possible, and 2) There was more noticeable isolated porosity and small oxide inclusions than previously seen in these materials. Again, by optimizing the closed loop feedback control system, features like this lack of uniformity can be overcome. The porosity did not appear to measurably degrade either the ductility or the strength. The oxide particles may originate in the powder feedstock.

Based on these observations, it appears that use of the LENS process to deposit 304L onto wrought material for modification or repair does provide adequate interface properties and microstructures equal to or better than the base material. Although additional qualification, definition of acceptance criteria, and process control enhancements are needed, the results of this work indicate that there are no apparent impediments to process qualification.

## **Acknowledgements:**

The authors would like to thank Mike Tootle for mechanical testing, Andy Garcia for metallographic sample preparation, and Jeff Chames for fractographic images.